RESEARCH ARTICLE

BORNEO SCIENCE
THE JOURNAL OF SCIENCE & TECHNOLOGY

Journal homepage: https://jurcon.ums.edu.my/ojums/index.php/borneo-science

FABRICATION AND CHARACTERIZATION OF CHITOSAN/TIO₂ MEMBRANES FOR SCENEDESMUS REMEDIATION: A PRELIMINARY STUDY

Mohamad Wafiuddin Ismail*[1], Husna Sophea Haszlihisham[2], Normawaty Mohammad Noor[3], Saiful Arifin Shafiee[4], Roziawati Mohd Razali[5] and Norazmi Ahmad[6]

*[1, 2, 4, 6] Department of Chemisty, Kulliyyah of Science, International Islamic University Malaysia, Pahang, Malaysia.
[3] Department of Marine, Kulliyyah of Science, International Islamic University Malaysia, Pahang, Malaysia
[5] Fisheries Research Institute Malaysia, Batu Maung, 11960 Bayan Lepas, Penang, Malaysia

*** Correspondence:**
wafisnj@iium.edu.my

Received: 23 February 2026
Revised: 26 May 2026
Accepted: 28 May 2026
Published online: 30 March 2026

Doi : 10.51200/bsj.v47i1.7401

ABSTRACT. *Excess nutrients from human activities have triggered harmful algal blooms (HABs), degrading water quality and ecosystem health. Traditional control methods like ultrasonication and chemical coagulants are limited by high costs and risks of secondary pollution. To address these challenges, this study investigates the use of polymeric membranes as a cost-effective and sustainable solution. In this preliminary study, porous chitosan/TiO_2 composite membranes were fabricated and evaluated as immobilized membrane materials for Scenedesmus removal. The purpose of the work was to establish the baseline performance of chitosan membranes containing immobilized TiO_2 and to compare the effect of TiO_2 loading on membrane-assisted algal removal. Fourier transform infrared spectroscopy (FTIR) confirmed the presence of chitosan functional groups and indicated TiO_2 incorporation through Ti-O-related absorption in the 467–457 cm^{-1} region. Thermogravimetric analysis (TGA) showed that TiO_2-containing membranes exhibited lower overall mass loss than the chitosan-only membrane, with the 1:2 chitosan/TiO_2 formulation showing the lowest reported total mass loss of 49.61%, suggesting the contribution of inorganic TiO_2 to the residual mass and thermal resistance of the composite. Scenedesmus removal was assessed by hemocytometer counting at 30 min, 1 h, 4 h, and 8 h. The processed average removal efficiencies were 37.64% for chitosan, 42.63% for 1:1 chitosan/TiO_2, and 60.56% for 1:2 chitosan/TiO_2. The observed removal is interpreted primarily as an overall membrane-assisted removal effect involving adsorption and physical entrapment within the porous chitosan scaffold, with a possible TiO_2 assisted contribution. The chitosan-based membranes demonstrated high algae removal efficiency, with chitosan alone achieving 37.64%, 1:1 chitosan/TiO_2 reaching 42.63%, and 1:2 chitosan/TiO_2 achieving the highest at 60.56%. The findings demonstrate the potential of porous chitosan/TiO_2 membranes as a preliminary platform for Scenedesmus mitigation and provide a basis for future mechanistic studies.*

Keywords:
Harmful algal blooms, chitosan, titanium dioxide, membrane, mitigation

INTRODUCTION

Algae, being photosynthetic organisms, are predominantly found in aquatic environments such as oceans, rivers, lakes, and ponds. They play a crucial role in oxygen production and have diverse applications in nutrition, pharmacology, and industry (Singh et al., 2023, Shabuddin et al., 2024). Algae exhibit a wide range of morphologies, from microscopic unicellular species to large multicellular forms reaching several meters in length. However, under favorable conditions, excessive algal growth can lead to the formation of harmful algal blooms (HABs) (Newton & Melaram, 2023; Khan et al., 2025).

A severe HAB event at Clear Lake, California, recorded microcystin toxin concentrations as high as 160,378 μg/L, posing serious threats to aquatic ecosystems and public health (Solomon et al., 2022). This alarming incident underscores the growing global threat of HABs, which contaminate water sources, disrupt aquatic ecosystems, and jeopardize public safety. The increasing occurrence of HABs is largely attributed to climate change, excessive nutrient loading, and other anthropogenic activities (Sarkar, 2018). One major anthropogenic driver of HAB formation is eutrophication, primarily caused by agricultural runoff, which enriches water bodies with nutrients, particularly nitrogen, thereby promoting algal overgrowth (Albou et al., 2024). These nutrients are washed into streams and rivers, creating favorable conditions for HAB proliferation (Lan et al., 2024).

According to UNESCO, approximately 300 species of microalgae are known to cause blooms, with around 75 of these producing harmful toxins. These toxins can be transmitted to humans through the consumption of contaminated seafood, resulting in health issues such as vomiting, diarrhea, and dizziness (Oh et al., 2023). Additionally, HABs contribute to widespread fish kills by depleting oxygen levels and obstructing light penetration, which hinders photosynthesis and leads to hypoxia. Such ecological disruptions also have severe economic impacts, particularly in communities reliant on fisheries. Consequently, various mitigation methods have been developed to control HABs. Conventional approaches such as ultraviolet (UV) radiation, ultrasonication, coagulant application, and the use of algicidal bacteria have demonstrated efficacy in reducing HAB levels. However, these methods face challenges including the potential release of harmful substances such as microcystins, high operational costs, and the generation of secondary contaminants in aquatic systems (Li et al., 2020).

Photocatalysis using titanium dioxide (TiO_2) nanoparticles has emerged as a promising strategy for algae mitigation due to its excellent photocatalytic activity, cost-effectiveness, and corrosion resistance (Natarajan et al., 2018). Nonetheless, practical application of TiO_2 under solar irradiation is limited by difficulties in separating the nanoparticles from treated water and concerns about their potential toxicity to aquatic life if released into the environment (He et al., 2020). These limitations can be addressed by immobilizing TiO_2 onto suitable support materials such as polymer films and porous polymers. Various polymers have been explored for this purpose in water treatment and antifouling applications. For example, poly(methyl methacrylate)-TiO_2 membranes have demonstrated significant photocatalytic activity, degrading up to 82.3% of methyl orange dye (Bhattacharyya et al., 2023), while polyethylene glycol-polyvinylidene fluoride/TiO_2 nanocomposite coatings have shown high efficiency in antifouling applications (Zhang et al., 2024).

This study investigates the effectiveness of TiO_2 immobilized on chitosan membranes for the removal of both harmful algae. To the best of our knowledge, no prior studies have examined the use of chitosan/TiO_2 composite membranes mitigation of HABs. Chitosan was selected as the membrane material due to its biocompatibility, biodegradability, and cost-effectiveness. Its porous structure has shown excellent performance in various water treatment applications, including oil/water separation (Su et al., 2017; Wang et al., 2024). The chitosan/TiO_2 composite membranes, prepared with a sponge like architecture, are hypothesized to effectively absorb harmful algae while preventing secondary contamination. In this system, the polymeric matrix absorbs the pollutants, and the embedded TiO_2 nanoparticles undergo photocatalytic reactions to generate reactive oxygen species, which degrade algal cells. The use of biodegradable polymers enhances environmental safety and sustainability, ensuring minimal ecological impact while maintaining high remediation efficiency. The present study focuses on

the fabrication, characterization, and preliminary evaluation of chitosan/TiO_2 composite membranes for Scenedesmus removal.

MATERIALS AND METHODS

MATERIALS

Chitosan powder medium molecular weight was acquired from Sigma Aldrich. Titanium dioxide (TiO_2) nanopowder with particle size <100 nm, acetic acid (CH_3COOH), sodium hydroxide (NaOH) and acetic acid were obtained from Sigma Aldrich. All chemicals were used as received without further purification.

METHODS

Fabrication of Chitosan/TiO_2 Composite Membranes

Chitosan/TiO_2 composite membranes with different ratios were fabricated and the amounts of chitosan and TiO_2 used in the preparation of each composite membrane are detailed in Table 1. Various ratios were employed to investigate the optimal incorporation of the TiO_2 in the membranes for the algae mitigation.

Table 1. Amounts of polymers used for chitosan/TiO2 composite membranes

Types	Amount used (g)	
	Chitosan	TiO_2
Chitosan	1.00	-
1:1 Chitosan/TiO_2	1.00	1.00
1:2 Chitosan/TiO_2	1.00	2.00

Accurately weighed amounts of chitosan powder and TiO_2 were mixed and dissolved in 50 mL of 1% (v/v) acetic acid to form solution A, which was then stirred for 1 hour. Separately, 2 g of NaOH was dissolved in 50 mL of deionized water to produce solution B. To synthesize the chitosan membrane, solution A was added to solution B slowly at room temperature, and the mixture was stirred at 350 rpm until a precipitate formed. The resulting precipitate was collected using filter paper, transferred into a petri dish, and frozen overnight at - 40 °C. The frozen chitosan sponge was subsequently freeze-dried at - 40 °C for 24 hours to obtain the final membrane.

Preparation of Scenedesmus Culture

The procedure began with the preparation of Bold's Basal Medium (BBM) following the method described by Lyod et al. (2021), followed by the autoclaving 1-L conical flasks for sterilization. The flask was then filled with 200 mL of BBM and 200 mL of Scenedesmus stock culture. Aeration was supplied to both flasks, which were covered with cotton wool and aluminum foil to minimize the risk of contamination. The cultures were incubated undisturbed for one week to promote algal growth. Algal cell density was monitored by counting the number of cells using a hemocytometer.

Scenedesmus Removal Experiment

The algae mitigation experiment was conducted in an autoclaved 100 mL beaker containing 50 mL of Scenedesmus culture. The culture was maintained at 24 h light cycle and temperature of ± 27oC. Membrane samples were cut to a uniform size of 1.5 cm x 1.5 cm. Each membrane type was tested with three replicates (n = 3) and one control (without membrane). The experiment evaluates overall membrane-assisted Scenedesmus removal under ambient laboratory/culture-light conditions. At selected time intervals (0 minutes, 30 minutes, 1 hour, 4 hours, and 8 hours), approximately 1 mL of the cell culture was withdrawn from a depth of 2 cm below the surface. Prior to sampling, the beakers were gently swirled to ensure homogeneity. Cell concentration of Scenedesmus was determined using a hemocytometer under a light microscope. For each sample, two 1 mL aliquots were counted, and the average cell count was calculated to enhance accuracy. The removal efficiency (RE) of each membrane in mitigating algae growth was calculated using Equation 1. where RE represents the removal efficiency of Scenedesmus cells (%), C_0 represents the initial cell concentration before membrane treatment (cells/mL), and C_t represents the cell concentration after treatment at time t (cells/mL). The treatment

time, t, refers to the sampling intervals of 30 min, 1 h, 4 h, and 8 h. Cell concentration was determined using a hemocytometer and reported as cells/mL

$$\text{RE (\%)} = \frac{c_0 - c_T}{c_0} \; x \; 100 \quad \text{(Equation 1)}$$

Composite Membrane Characterization

Fourier Transform Infrared Spectroscopy (FTIR)

FTIR analysis was conducted to investigate the chemical structure of the membranes and to confirm the successful incorporation of TiO_2, indicated by the presence of Ti–O stretching vibration peaks. The instrument used was a PerkinElmer Frontier FTIR spectrometer. Spectra were recorded over the range of 400–4000 cm^{-1}. Membrane samples were finely ground and mixed with potassium bromide (KBr) at a ratio of 1:20. The homogenized mixture was placed into a pellet die and subjected to a pressure of 10 tons using a hydraulic press to form a pellet. The FTIR spectrum of the sample was then recorded.

Thermogravimetric Analysis (TGA)

Thermogravimetric analysis (TGA) was performed to assess the thermal stability and decomposition behavior of the composite membranes. A Shimadzu TGA-50 Thermogravimetric Analyzer was used for the analysis. The temperature was programmed to increase from 25 °C to 700 °C at a heating rate of 10 °C/min. A constant gas flow of 50 mL/min was maintained to ensure a stable inert atmosphere during the analysis.

Scanning Electron Microscopy (SEM)

SEM analysis was used to examine the surface morphology, porosity, and dispersion of TiO_2 particles within the polymer matrix. A Carl Zeiss AG EVO 50 scanning electron microscope was employed for the imaging. Prior to analysis, the samples were coated with a thin layer of gold to enhance conductivity and image quality.

RESULTS AND DISCUSSION

Development of Porous Chitosan/TiO_2 Composite Membranes

Chitosan/TiO_2 composite membranes were prepared using the phase inversion method followed by freeze-drying to promote porosity. Initially, the chitosan solution (Solution A) was stirred for 1 hour to ensure complete dissolution. Upon adding Solution B to this acidic chitosan solution, rapid coagulation occurred due to ionic cross-linking, leading to the precipitation of chitosan. This process is driven by the deprotonation of the amino groups on chitosan upon exposure to a basic medium such as NaOH (Kou et al., 2021). The precipitated chitosan/TiO_2 coagulant was then frozen overnight and subsequently subjected to freeze-drying. Freeze-drying facilitated the formation of a porous, sponge-like architecture through the sublimation of ice crystals formed during freezing, yielding a macroporous matrix ideal for absorption applications (Guastaferro et al., 2021). This morphology is relevant for algal-removal applications because pores and internal channels can increase the opportunity for algal cells to contact the membrane and become physically retained.

The cross-sectional morphology of the resulting chitosan/TiO_2 membranes, as shown in Figure 1, revealed a layered structure with well-defined porosity, indicating enhanced surface area and potential for increased adsorption and photocatalytic activity. Notably, membranes fabricated with varying TiO_2 loadings did not exhibit significant morphological differences in terms of layer formation and thickness, which remained consistent across all formulations. This observation is in line with previous findings where TiO_2 incorporation at moderate concentrations did not significantly alter the structure of chitosan-based membranes (Xing et al., 2020).

Figure 1. Cross-sectional image of the chitosan/TiO_2 composite membrane showing the porous sponge-like architecture generated after freeze-drying.

Fourier Transform Infrared Spectroscopy (FTIR) was employed to confirm the incorporation of TiO_2 into chitosan composite membranes. The FTIR spectra of pure chitosan, 1:1 chitosan/TiO_2, and 1:2 chitosan/TiO_2 composites are presented in Figure 2. Chitosan shows characteristic absorption bands associated with its functional groups. The broad absorption peak observed at 3400–3200 cm^{-1} is assigned to the overlapping stretching vibrations of hydroxyl (–OH) and amine ($–NH_2$) groups. The amide I band appears at approximately 1635 cm^{-1}, while the amide II band is observed near 1401 cm^{-1}, indicating the presence of C=O stretching and N–H bending vibrations, respectively. A distinct band near 1117 cm^{-1} corresponds to asymmetric C–O–C stretching vibrations, characteristic of the polysaccharide backbone. These peaks were consistently observed in all chitosan-containing samples, indicating the retention of the polymer's primary functional groups after TiO_2 incorporation.

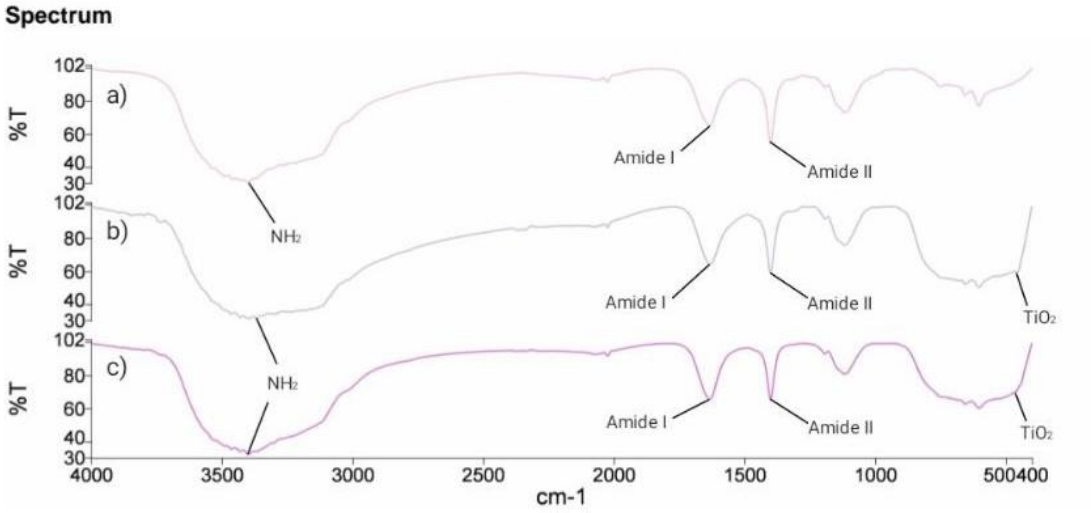

Figure 2. FTIR spectra for (a) chitosan, (b) 1:1 chitosan/TiO_2, and (c) 1:2 chitosan/TiO_2.

For the chitosan/TiO_2 composite membranes, an additional absorption feature in the 467–457 cm^{-1} region was observed and is assigned to Ti-O vibration from the TiO_2 lattice (Spoială et al., 2022). The presence of this band supports the incorporation of TiO_2 into the chitosan matrix. An increase in Ti-O band intensity with higher TiO_2 content is consistent with the greater TiO_2 loading in the 1:2 formulation. The interaction between chitosan and TiO_2 may also lead to minor shifts or changes in the intensity of the characteristic peaks due to potential hydrogen bonding or electrostatic interactions between the TiO_2 and chitosan. Previous studies have shown that the Ti–O–C or Ti–O–N bonds can be formed between TiO_2 and chitosan, further supporting their compatibility in composite formation (Habiba et al., 2019).

Thermogravimetric analysis (TGA) was performed to assess the thermal stability of pure chitosan and chitosan/TiO_2 composite membranes (Figure 3). The pristine chitosan membrane showed an initial mass-loss event beginning around 59.04 °C. This low-temperature event is attributed primarily to moisture evaporation and removal of physically adsorbed water rather than polymer backbone decomposition. Chitosan is hydrophilic because of its hydroxyl and amine groups, which can retain water through hydrogen bonding (Hussein et al., 2021). The main thermal-degradation region of chitosan occurs at higher temperature, commonly above approximately 200 °C, and is associated with degradation of the polysaccharide backbone, cleavage of glycosidic linkages, and release of volatile decomposition products (Mallakpour & Madani, 2015).

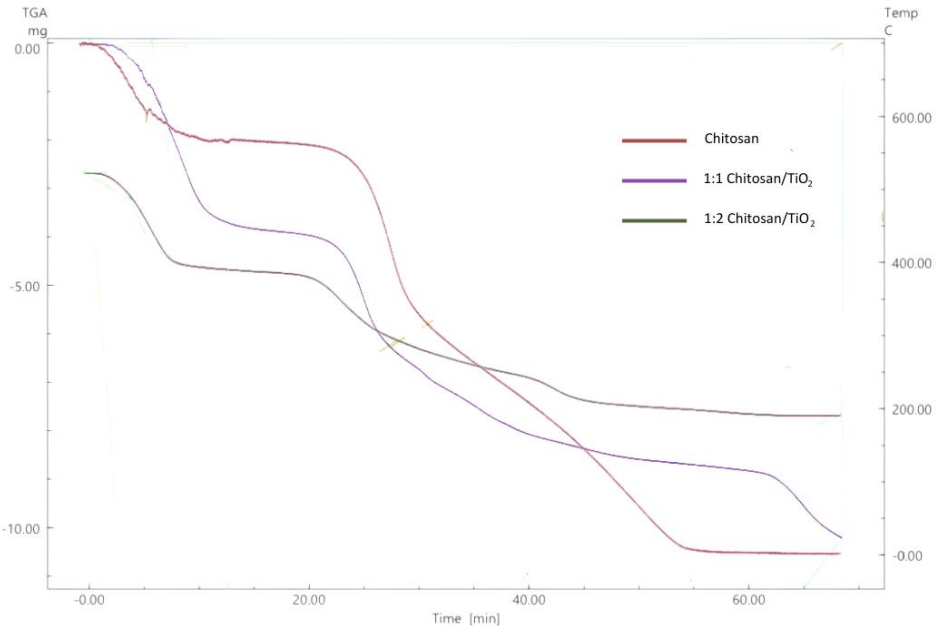

Figure 3. TGA spectra for chitosan, 1:1 chitosan/TiO_2, and 1:2 chitosan/TiO_2.

Upon incorporation of TiO_2, a notable enhancement in thermal stability was observed. The pristine chitosan membrane showed a high total mass loss of 89.36%, while the TiO_2-containing membranes showed lower total mass losses. The 1:1 chitosan/TiO_2 membrane showed a total mass loss of 57.29%, and the 1:2 chitosan/TiO_2 membrane showed the lowest total mass loss of 49.61%. The lower mass loss of the composite membranes is attributed to the inorganic TiO_2 fraction, which remains as thermally stable residue at high temperature, and to possible physical interactions between TiO_2 particles and chitosan chains. TiO_2 may restrict polymer-chain mobility and act as a heat-resistant inorganic component within the matrix (Hussein et al., 2021). The higher residual mass of the 1:2 chitosan/TiO_2 membrane is consistent with its higher TiO_2 loading. Similar trends have been reported for chitosan/TiO_2 systems, where TiO_2 incorporation increased residual mass and improved the apparent thermal resistance of the composite material (Becenan & Erdogan, 2022). TiO_2 incorporation into polymeric composites limits the volatilization of degradation products and insulates the polymer from further decomposition.

Scenedesmus Removal Performance

The Scenedesmus removal efficiencies of the chitosan, 1:1 chitosan/TiO_2, and 1:2 chitosan/TiO_2 membranes are summarized in Table 2 and illustrated in Figure 4. The data are reported as processed average removal efficiencies obtained under culture-light conditions. The pristine chitosan membrane exhibited lowest removal efficiency at an average of 37.64% compared to other membranes. This performance is attributed mainly to physical adsorption and entrapment of algal cells within the porous membrane structure. While the sponge-like morphology can retain cells through pore capture and surface adhesion, the presence of amine groups in chitosan promotes electrostatic interactions with the negatively charged algal cell membranes, enhancing retention (Park et al., 2020). The gradual increase

in removal efficiency suggests that although the membrane is effective, its adsorption capacity is reached at a slower rate.

Table 2. Scenedesmus removal efficiency of chitosan/TiO_2 composite membranes.

Types	Removal Efficiency (%)				
	30 min	1 hr	4 hrs	8 hrs	Average
Chitosan	5.27±9.79	26.36±12.08	60.76±11.91	58.17±5.35	37.64
1:1 Chitosan/TiO_2	5.27±12.47	26.36±16.52	60.76±5.66	78.84±2.84	42.63
1:2 Chitosan/TiO_2	53.03±3.56	58.76±3.47	57.17±5.01	73.26±1.68	60.56

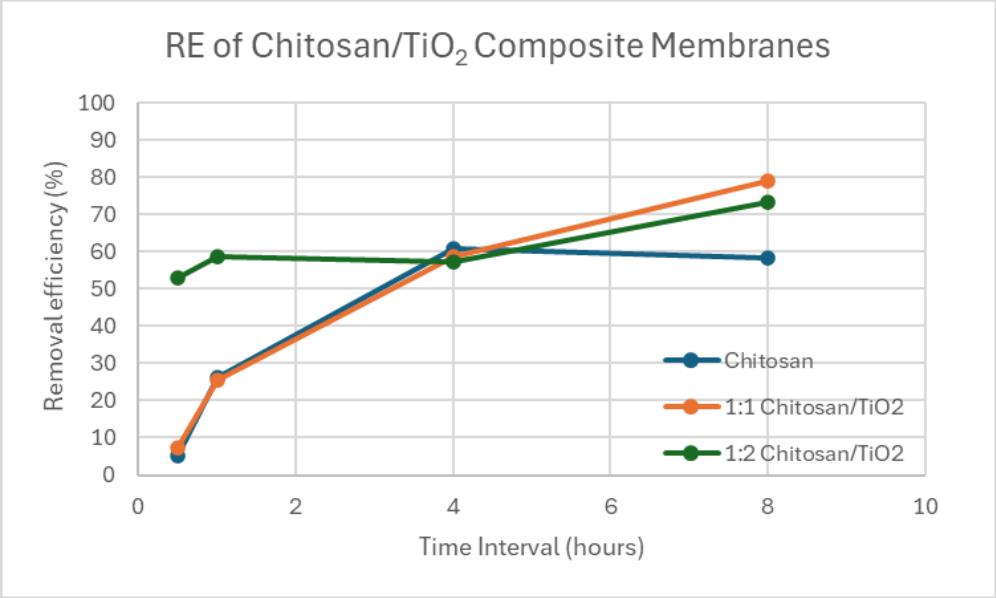

Figure 4. Scenedesmus removal efficiency of chitosan/TiO_2 composite membranes.

The incorporation of TiO_2 into the chitosan matrix significantly improved the removal performance. The 1:1 chitosan/TiO_2 membrane showed a slightly higher average removal efficiency of 42.63%, while the 1:2 chitosan/TiO_2 membrane showed the highest processed average removal efficiency of 60.56%. The improved performance of the TiO_2 containing membranes may be related to several factors, including additional inorganic surface sites, changes in membrane texture, and possible light assisted TiO_2 contribution under ambient culture light conditions. The 1:2 chitosan/TiO_2 membrane reached 53.03% removal as early as 30 min, suggesting rapid interaction between the algae suspension and the composite membrane. At later time points, the removal profile did not increase linearly at every interval, which may reflect sampling variability, cell aggregation, partial release of physically retained cells, or local differences in suspension homogeneity.

The performance of the membranes in this study can also be compared to previous work. Ibrahim et al. (2022) reported a removal efficiency of 76.1% over 72 hours using hybrid chitosan-modified TiO_2 films against Alexandrium minutum. In contrast, the 1:2 chitosan/TiO_2 membrane developed in this study achieved a comparable removal efficiency in only 8 hours, indicating a significantly faster removal rate. This difference may be attributed to differences in membrane morphology. Ibrahim et al.'s membranes, prepared via phase inversion technique, exhibited a dense and smooth structure, with TiO_2 nanoparticles embedded near the surface. Compact morphology limits active site accessibility and mass transfer. In contrast, the membranes in this study were fabricated using a freeze-drying method, resulting in a sponge-like, highly porous structure. This morphology offers a substantially larger surface area and better internal diffusion pathways, allowing greater contact between TiO_2 particles and algal cells. Furthermore, Natarajan et al. (2018) reported that a chitosan/TiO_2/Ag composite film achieved an algae viability reduction of 45.42 ± 0.36%. The 1:2 chitosan/TiO_2 membrane in the present study shows better results, likely due to its highly porous structure, which enhances algal entrapment.

Scanning Electron Microscopy (SEM) images were used to examine the morphology of the chitosan and chitosan/TiO_2 membranes (Figure 5). The images show a porous, sponge like structure with interconnected voids and layered features. This morphology is consistent with the freeze-drying process, where ice crystal formation and subsequent sublimation create pores and internal channels (Guastaferro et al., 2021).

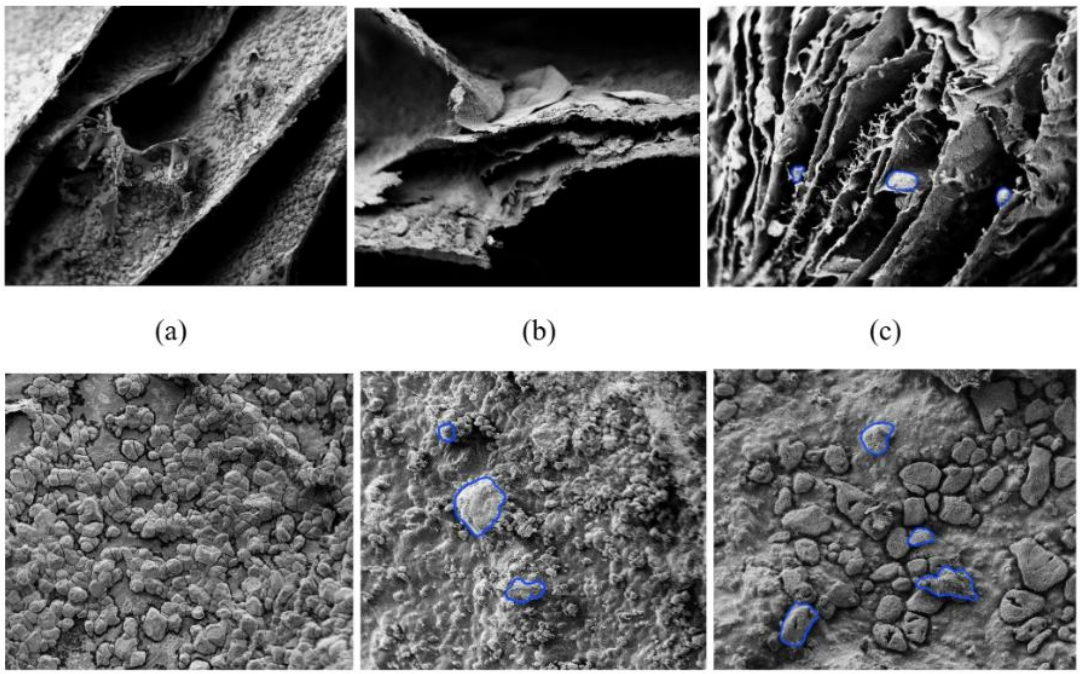

Figure 5. SEM images of (a) chitosan, (b) 1:1 chitosan/TiO2, (c) 1:2 chitosan/TiO2, above; cross-sectional at 100x magnification, bottom; surface at 300x magnification.

The resulting porous architecture is particularly advantageous for applications involving adsorption, as it promotes greater contact between the active membrane surface and target pollutants. The interconnected pore network enhances mass transport, facilitates diffusion of algal cells into the membrane structure, and improves retention capacity (Ikono et al. 2019), on the chitosan-TiO_2 composites. Particle like features are visible in the TiO_2 containing membranes, suggesting the presence of embedded inorganic particles within the chitosan matrix, which display distinct particle like features embedded within the pore walls. These features are indicative of successful TiO_2 incorporation into the biopolymeric scaffold. Uniform distribution of TiO_2 within the porous matrix is crucial, as it ensures that the potential photocatalytic sites are accessible to light and pollutants, thereby maximizing the generation of reactive oxygen species under light exposure. This incorporation is assumed to lead to improved photocatalytic efficiency and mechanical integrity of the newly developed membrane (Spoială et al., 2022; Esparza et al., 2020). Additionally, the morphology of the membrane plays a vital role in influencing not only physical adsorption but also light penetration. Open, porous structures allow deeper light penetration and more efficient utilization of embedded TiO_2, which is often a limitation in dense or non-transparent membranes

CONCLUSION

Porous chitosan/TiO_2 composite membranes were successfully fabricated using an alkaline precipitation and freeze drying approach and were preliminarily evaluated for Scenedesmus removal. FTIR analysis indicated the retention of chitosan functional groups and the incorporation of TiO_2 through Ti-O-related absorption bands. TGA showed reduced total mass loss and higher residual mass in TiO_2-containing membranes, particularly the 1:2 chitosan/TiO_2 membrane, reflecting the contribution

of the thermally stable inorganic component. SEM observations confirmed a porous, sponge-like morphology that is favourable for contact and physical retention of algal cells.

The algae removal test showed that the 1:2 chitosan/TiO_2 membrane achieved the highest processed average removal efficiency of 60.56% within the 8 h evaluation period, followed by the 1:1 chitosan/TiO_2 membrane and the pristine chitosan membrane. These findings suggest that increasing TiO_2 loading may improve the overall membrane assisted removal performance. The main experimentally supported mechanism is physical entrapment/adsorption by the porous chitosan based membrane, while TiO_2 assisted effects remain possible but require further verification. Future work should focus on controlled photocatalytic testing, mechanistic controls, quantitative porosity, TiO_2 leaching, reusability, mechanical stability, kinetic modelling, and ecotoxicity assessment before practical environmental application.

ACKNOWLEDGEMENT

International Islamic University Malaysia and the Department of Fisheries for supported this research (12th Malaysia Plan Development Fund (22501-509).

REFERENCES

Albou, E.M., Abdellaoui, M., Abdaoui, A., Boughrous, A.A. 2024. Agricultural Practices and their Impact on Aquatic Ecosystems – A Mini-Review. *Ecological Engineering & Environmental Technology*, 25(1); 321-331.

Becenen, N. Erdogan S. 2022. Chitosan and nano-TiO_2 coating improves the flame retardancy of dyed and undyed denim fabrics by increasing the charring. *Journal of Industrial Textiles*, 51(1); 1252S-1278S

Bhattacharyya, S., Algieri, C., Davoli, M., Calabrò, V., Chakraborty, S. 2023. Polymer-based TiO_2 membranes: An efficient route for recalcitrant dye degradation. *Chemical Engineering Research and Design*, 193; 641–648.

Esparza, L.M., Gomez, J.M.R., Verdugo, C.I.M., Silva, N.G., Toledo, R.R., Aguirre, S.A., Larios, A.P. Gonzalez E.M. 2020. Chitosan-TiO_2: A Versatile Hybrid Composite. *Materials*, 13(4); 811.

Guastaferro, M., Baldino, L., Reverchon, E., Cardea, S. 2021. Production of Porous Agarose-Based Structures: Freeze-Drying vs. Supercritical CO_2 Drying. *Gels*, 7(4); 198.

Habiba, U., Joo, T.C., Shezan, S.K.A., Das, R., Ang, B.C. Afifi, A.M. 2019. Synthesis and characterization of chitosan/TiO_2 nanocomposite for the adsorption of Congo red. *Desalination and Water Treatment*, 164; 361-367.

He, X., Wang, A., Wu, P., Tang, S., Zhang, Y., Li, L., Ding, P. 2020. Photocatalytic degradation of microcystin-LR by modified TiO_2 photocatalysis: A review. *Science of the Total Environment*, 743.

Hussein, E.M., Desoky, W.M., Hanafy, M.F., Guirguis, O.W. 2021. Effect of TiO_2 nanoparticles on the structural configurations and thermal, mechanical, and optical properties of chitosan/TiO_2 nanoparticle composites. *Journal of Physics and Chemistry of Solids*, 152; 109983.

Ibrahim, N.H., Iqbal, A., Mohammad-Noor, N., Razali, R.M., Sreekantan, S., Yanto, D.H.Y., Mahadi, A.H., Wilson, L.D. 2022. Photocatalytic Remediation of Harmful Alexandrium minutum Bloom Using Hybrid Chitosan-Modified TiO_2 Films in Seawater: A Lab-Based Study. *Catalysts,* 12(7).

Ikono, R., Li, N., Pratama, N.H., Vibriani, A., Yuniarni, D.R., Luthfansyah, M., Bachtiar, B.M., Bachtiar, E.W., Mulia, K., Nasikin, M., Kagami, H., Li, X., Mardliyati, E., Rochman, N.T., Nagamura-Inoue, T., Tojo, A. 2019. Enhanced bone regeneration capability of chitosan sponge coated with TiO_2 nanoparticles. *Biotechnology Reports*, 24; e00350.

Khan, N., Bhowmilk, P.P., Sarker, M.S., Yang, H., Li, R. Liu, J. 2025. Impact of water quality parameters on harmful algal bloom mitigation and phosphorus removal by lab-synthesized $\gamma Fe_2O_3/TiO_2$ magnetic photocatalysts. *Algal Research*, v86; 103932.

Kou, S., Peters, L M., Mucalo, M.R. 2021. Chitosan: A review of sources and preparation methods. *International Journal of Biological Macromolecules*, 169; 85–94.

Lan, J., Liu, P., Hu, X., Zhu, S. 2024. Harmful Algal Blooms in Eutrophic Marine Environments: Causes, Monitoring, and Treatment. *Water*, 16(17), 2525.

Li, S., Tao, Y., Zhan, X. M., Dao, G. H., & Hu, H. Y. (2020). UV-C irradiation for harmful algal blooms control: A literature review on effectiveness, mechanisms, influencing factors and facilities. *Science of The Total Environment*, 723, 137986.

Lyod, C., Tan, K.H., Lim, K.L., Valu, V.G., Fun, S.M.Y, Chye, T.R., Mak, H.M., Sim, W.X., Musa, S.L., Ng, J.J., Nordin, N.S., Aidil, N.M., Eng, Z.Y.W., Manickavasagam, P. New, J.Y. 2021. Identification of microalgae cultured in Bold's Basal medium from freshwater samples, from a high-rise city. *Scientific Reports*, v11: 4474.

Mallakpour, S., Madani, M. 2015. Effect of Functionalized TiO_2 on Mechanical, Thermal and Swelling Properties of Chitosan-Based Nanocomposite Films. *Polymer-Plastics Technology and Engineering*, 54(10); 1035–1042.

Natarajan, S., Lakshmi, D.S., Thiagarajan, V., Mrudula, P., Chandrasekaran, N., Mukherjee, A. 2018. Antifouling and anti-algal effects of chitosan nanocomposite (TiO_2/Ag) and pristine (TiO_2 and Ag) films on marine microalgae Dunaliella salina. *Journal of Environmental Chemical Engineering*, 6(6); 6870–6880.

Newton, A.R. Melaram, R. 2023. Harmful algal blooms in agricultural irrigation: risks, benefits, and management. *Water*, 5:1325300.

Oh, J.W., Pushparaj, S.S.C., Muthu, M., Gopal, J. 2023. Review of Harmful Algal Blooms (HABs) Causing Marine Fish Kills: Toxicity and Mitigation. *In Plants*, 12(23).

Park, Y.H., Kim, S., Kim, H.S., Park, C., Choi, Y.E. 2020. Adsorption Strategy for Removal of Harmful Cyanobacterial Species Microcystis aeruginosa Using Chitosan Fiber. *Sustainability*, 12(11), 4587.

Sarkar, S. K. 2018. *Algal blooms: Basic concepts. In Marine algal bloom: Characteristics, causes, and climate change impacts* (pp. 1-52). Springer.

Shabuddin, S.H., Noor, M.N., Ahmad, M.N., Iqbal, A. Ismail, M.W. 2024. Development of PCL/PMMA and PCL/PEG polymeric film as potential for algae removal. *Sains Malaysiana*, 53 (6).

Singh, V.K., Jha, S., Rana, P., Mishra, S., Kumari, N., Singh, S.C., Anand, S., Upadhye, V., Sinha, R.P. 2023. Resilience and Mitigation Strategies of Cyanobacteria under Ultraviolet Radiation Stress. *International Journal of Molecular Sciences*, 24(15); 12381.

Solomon, G.M., Stanton, B., Ryan, S., Little, A., Carpenter, C., Paulukonis, S. 2022. Notes from the Field: Harmful Algal Bloom Affecting Private Drinking Water Intakes - Clear Lake, California, June–November 2021. *Morbidity and Mortality Weekly Report*; 71(41), 1306.

Su, C., Yang, H., Zhao, H., Liu, Y., Chen, R. 2017. Recyclable and biodegradable superhydrophobic and superoleophilic chitosan sponge for the effective removal of oily pollutants from water. *Chemical Engineering Journal*, 330; 423–432.

Spoială, A., Ilie, C.I., Dolete, G., Croitoru, A.M., Surdu, V.A., Trușcă, R.D., Motelica, L., Oprea, O.C., Ficai, D., Ficai, A., Andronescu, E., Dițu, L.M. 2022. Preparation and Characterization of Chitosan/TiO2 Composite Membranes as Adsorbent Materials for Water Purification. *Membranes,* 12(8).

Wang, Y., Feng, X., Ke, Y., Mo, J., Lin, J., Wang, J., Zhou, C., Gan, F., Wang, L., Ma, C. 2024. Silicone decorated polycaprolactone electrospun fibrous membranes for oil/water separation. *The Journal of The Textile Institute*, 115(5); 744–756.

Xing, Y., Li, X., Guo, X., Li, W., Chen, J., Liu, Q., Xu, Q., Wang., Yang, H., Shui, Y. Bi, X. 2020. Effects of Different TiO2 Nanoparticles Concentrations on the Physical and Antibacterial Activities of Chitosan-Based Coating Film. *Nanomaterials*, 10; 1365.

Zhang, C.M., Qiu, Y.Z., Wu, H., Guan, J., Wang, S.G., & Sun, X.F. 2024. Polyethylene glycol-polyvinylidene fluoride/TiO2 nanocomposite polymer coatings with efficient antifouling strategies: Hydrophilized defensive surface and stable capacitive deionization. *Journal of Colloid and Interface Science*, 666; 585–593.